Supplemental Materials for "Emergence of flat bands and their impact on superconductivity in $Mo_5Si_{3-x}P_x$"

Rustem Khasanov,[1,*] Bin-Bin Ruan,[2,†] Yun-Qing Shi,[2,3] Gen-Fu Chen,[2,3] Hubertus Luetkens,[1] Zhi-An Ren,[2,3] and Zurab Guguchia[1]

[1]*Laboratory for Muon Spin Spectroscopy, Paul Scherrer Institute, CH-5232 Villigen PSI, Switzerland*
[2]*Institute of Physics and Beijing National Laboratory for Condensed Matter Physics, Chinese Academy of Sciences, Beijing 100190, China*
[3]*School of Physical Sciences, University of Chinese Academy of Sciences, Beijing 100049, China*

I. SAMPLE PREPARATION

The polycrystalline samples of $Mo_5Si_{3-x}P_x$ were prepared by solid state reaction in a way described in Ref. 1. The procedure included the initial mixing and pressing the elemental powders of Mo (99.9% purity), Si (99.999% purity), and P (99.99% purity) into pellets followed by two subsequent annealing at 1073 K for 24 hours and at 1923 K for 20 hours.

II. CALCULATION DETAILS

First-principles calculations were performed based on the density functional theory (DFT), using the Quantum ESPRESSO package[2]. The generalized gradient approximation of Perdew-Burke-Ernzerhof (PBE) exchange correlation functionals were applied[3]. The optimized norm-conserving pseudopotentials were chosen[4]. The energy cutoffs for wavefunction and charge densities were 50 Ry and 400 Ry, respectively. Before each calculation, the cell dimensions and atomic positions were fully relaxed till each atom felt a force of less than 1×10^{-4} Ry Bohr^{-1}. Phosphorous doping was treated by the virtual crystal approximation (VCA), whose validation had been checked in Ref. 1. Monkhorst-Pack grids of $11\times11\times7$ and $21\times21\times15$ were used to calculate the charge densities and the density of states (DOS), respectively. No Hubbard parameters or spin-orbit coupling effects was taken into account, as they introduced no obvious change to the electronic band structure and DOS, as demonstrated in Ref. 1.

III. X-RAY DIFFRACTION MEASUREMENTS

The room temperature powder x-ray diffraction (XRD) data were collected on a PAN-analytical x-ray diffractometer with Cu-K_α radiation. Rietveld refinements were carried out using the GSAS package.[5] XRD patterns of polycrystalline $Mo_5Si_{3-x}P_x$ ($0\leq x\leq1.6$) are presented in Figure 1 (a). The main peaks were identified with the W_5Si_3 type structure (space group $I4/mcm$). The peaks marked by asterisks correspond to the impurity Mo_3P fraction.

A successful phosphorus doping into the Mo_5Si_3 matrix is confirmed by the corresponding changes of $a-$ and $c-$lattice constants, Fig. 1 (b). The phosphorus content in synthesized $Mo_5Si_{3-x}P_x$ samples was determined by comparing the lattice parameters a and c with those reported in Ref. 1. Figure 1 (c) implies that the measured P concentrations agree well with the nominal ones. Consequently, the nominal phosphorus content x was used for representing the data in the main text.

IV. RESISTIVITY MEASUREMENTS

The resistivity data were collected on a physical property measurement system (PPMS, Quantum Design). Figure 2 shows the resistivity curves normalized to the values at $T=16$ K $[R(T)/R(16\text{ K})]$ measured in magnetic fields ranging from 0.0 to 9.0 T. The superconducting transition temperature at the applied field $\mu_0H_{\rm ap}$ $[T_{\rm c}(\mu_0H_{\rm ap})]$ was determined as a cross point of $R(T,H_{\rm ap})(T)$ curve with $R(T)/R(16\text{ K})=0.5$ line, see the top left panel of Fig. 2.

V. SPECIFIC HEAT MEASUREMENTS

The specific heat ($C_{\rm p}$) measurements were performed by using the relaxation method on the same PPMS system as for resistivity experiments. The temperature dependencies of $C_{\rm p}$ of $Mo_5Si_{3-x}P_x$ are presented in Fig. 3 (a). Note

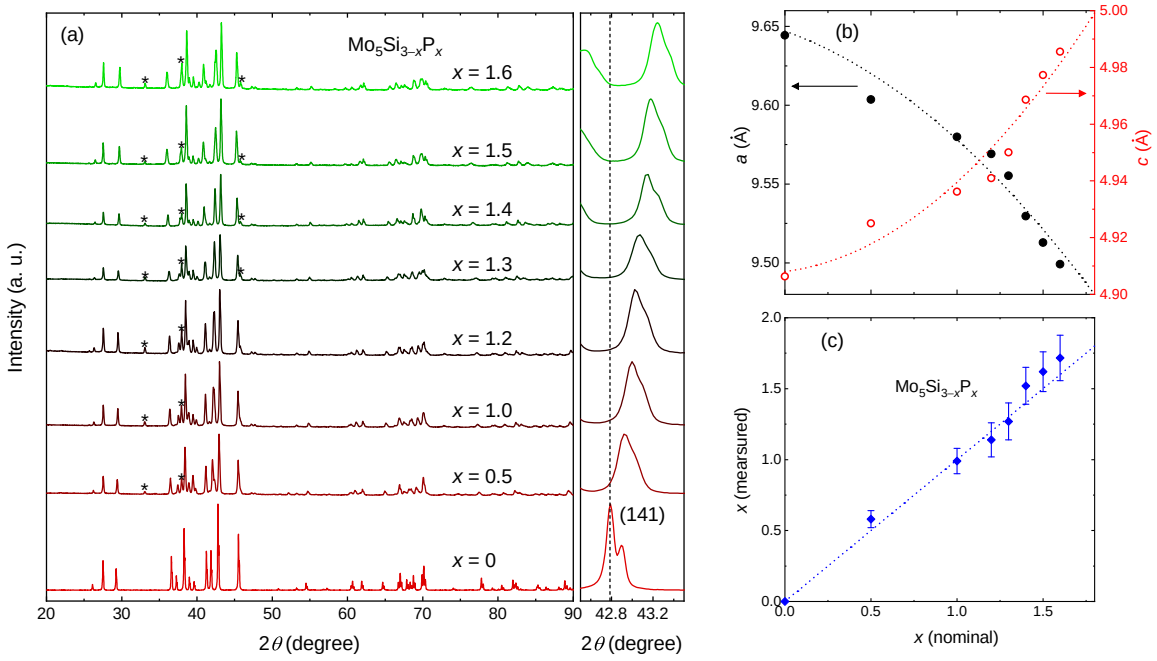

FIG. 1: (a) Powder x-ray diffraction patterns of $Mo_5Si_{3-x}P_x$ ($0 \leq x \leq 1.6$). The peaks of Mo_3P impurity phase are marked by asterisks. The inset shows the position of (141) peak of $Mo_5Si_{3-x}P_x$ at various doping levels. (b) Dependence of the lattice parameters a and c on the nominal phosphorus content x. (c) The measured phosphorus content versus their nominal value. The dash line represents the case where the measured values are equal to the nominal ones.

that, the $C_p(T)$ data were corrected by subtracting the minor contributions of Mo_3P.[1]

The temperature evolution of C_p in the normal state (*i.e.* for $T_c < T \lesssim 16$ K) was analyzed within the framework of the Debye model:

$$C_p(T) = \gamma T + \beta T^3 + \delta T^5, \tag{1}$$

where the linear T term represents the electronic specific heat contribution γ, while T^3 and T^5 terms account for the harmonic and anharmonic phonon contributions, respectively. Fits of the Debye model to $C_p(T)$ data are presented in Fig. 3 (a) by dotted lines.

The Debye temperature Θ_D was further obtained by using the 'harmonic' term β as:

$$\Theta_D = (12\pi^4 NR/5\beta)^{1/3}. \tag{2}$$

Here N is the number of atoms per formula unit, and R is the ideal gas constant. The dependence of Θ_D on x is shown in Fig. 3 (b).

The electron-phonon coupling constant λ_{ep} [Fig. 3 (c)] was estimated from the McMillan equation:[6]

$$\lambda_{ep} = \frac{1.04 + \mu^* \ln(\Theta_D/1.45T_c)}{(1 - 0.62\mu^*)\ln(\Theta_D/1.45T_c) - 1.04} \tag{3}$$

by using the Coulomb screening parameter $\mu^* = 0.13$.[1]

VI. DOPING DEPENDENCE OF THE DENSITY OF STATES

The absence of a competing ordered state(s), which might be responsible for reducing the number of carriers accessible for the superconducting condensate, was checked by comparing the Density of States (DOS) as they obtained from the first principle calculations [Fig. 4 (a)] with DOS at the Fermi level [$N(E_F)$] determined from the above reported quantities (γ and λ_{ep}) via:

$$\gamma = \frac{1}{3} N(E_F)\pi^2 k_B^2 (1 + \lambda_{ep}). \tag{4}$$

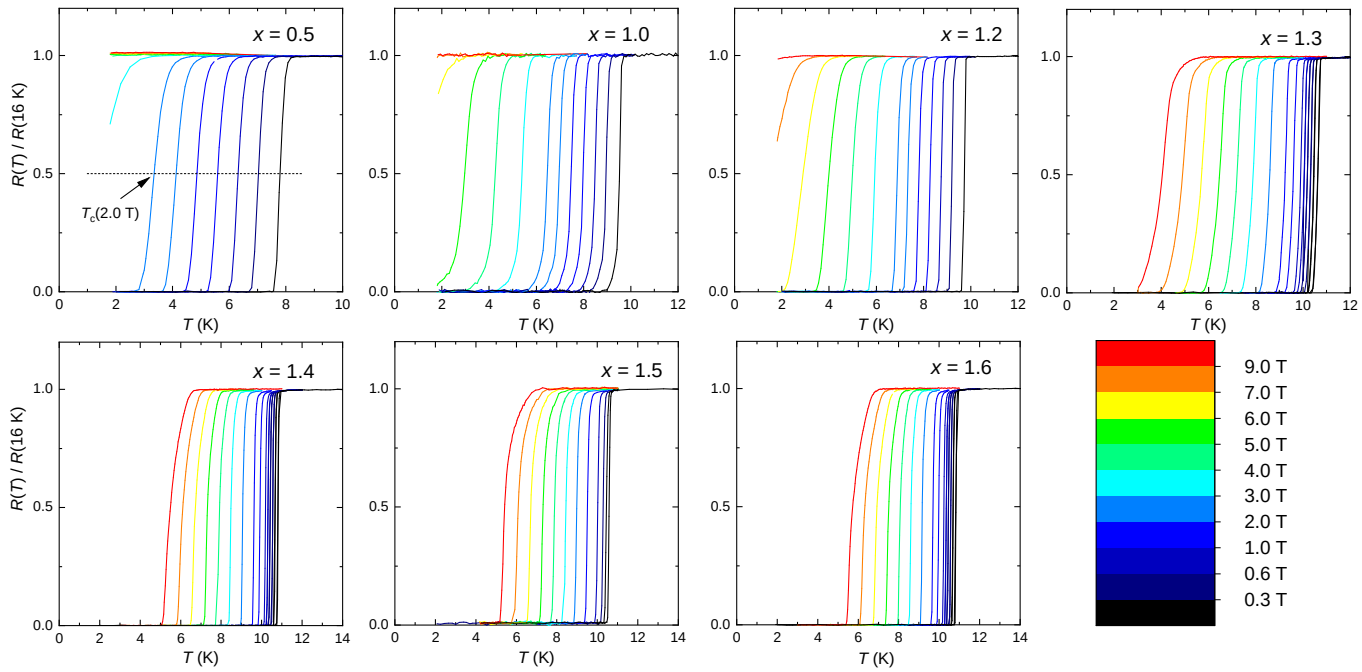

FIG. 2: Temperature dependencies of resistivity of $Mo_5Si_{3-x}P_x$ under magnetic fields ranging from 0.0 to 9.0 T. The superconducting transition temperature T_c is defined from the mid point of $R(T, H_{ap})$ curves [*i.e.* as the value where $R(T)/R(16\,K) = 0.5$, see the top left panel].

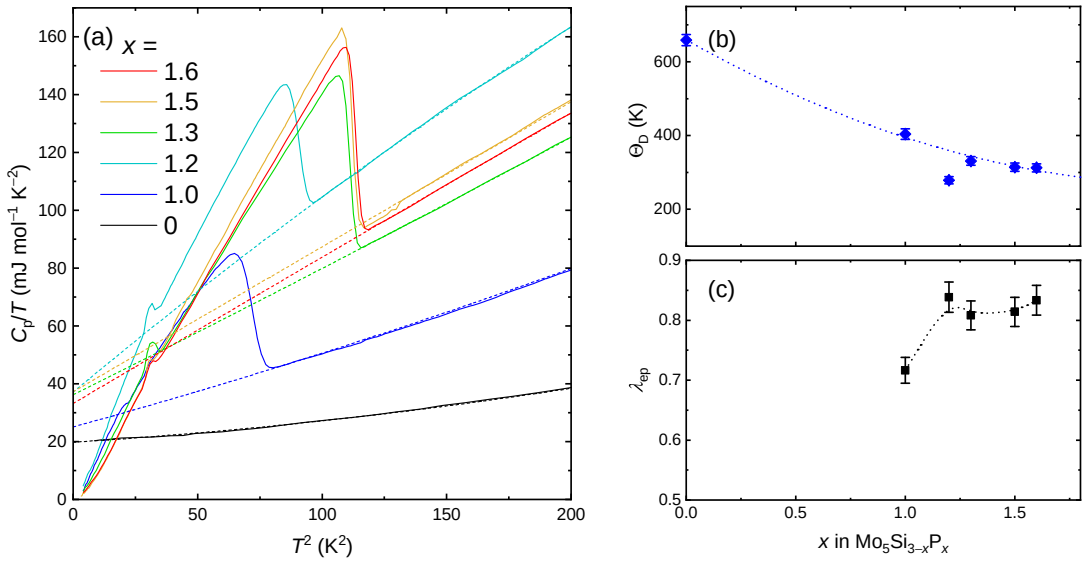

FIG. 3: (a) Temperature dependencies of the specific heat C_p of $Mo_5Si_{3-x}P_x$ under zero magnetic field. The dash lines correspond to the fit of the Debye model (Eq. 1) to the $C_p(T)$ data. The kinks at $T^2 \simeq 30$ K arise from the Mo_3P impurity. (b) Dependence of the Debye temperature (Θ_D) on the phosphorus content x. (c) Dependence of the electron-phonon coupling constant (λ_{ep}) on x.

An agreement between the 'theoretical' and the 'experimental' dependencies of $N(E_F)$ on x, as presented in Fig. 4 (b), confirms the absence of competing states formed above the superconducting transition temperature T_c.

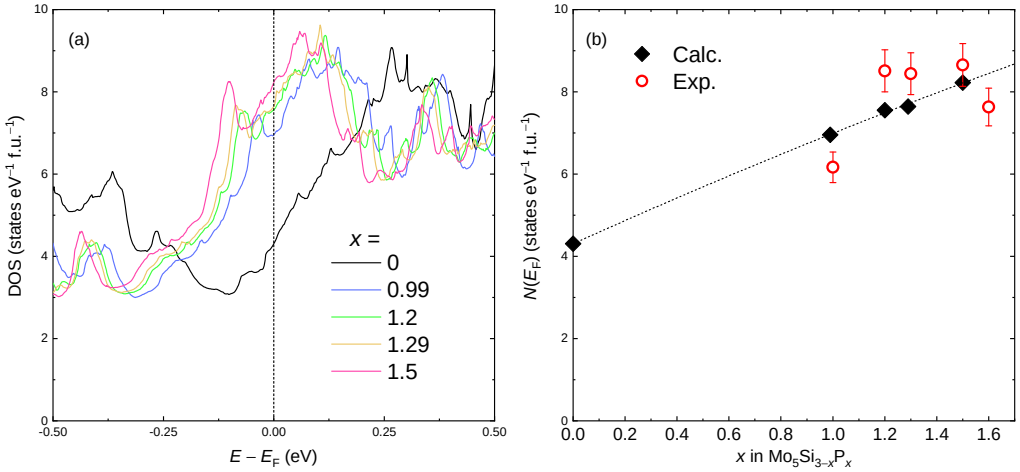

FIG. 4: (a) Calculated density of states (DOS) of $Mo_5Si_{3-x}P_x$ near the Fermi level (E_F). (b) Comparison of the calculated and experimental DOS on E_F [$N(E_F)$] of $Mo_5Si_{3-x}P_x$.

VII. μSR MEASUREMENTS

The muon-spin rotation/relaxation (μSR) measurements were carried out at the πM3 beam line by using GPS (General Purose Surface) μSR spectrometer (Paul Scherrer Institute, Villigen, Switzerland).[7] The zero-field (ZF) and transverse-field (TF) μSR measurements were performed at temperatures ranging from $\simeq$ 1.5 to 20 K. The typical counting statistics were $\sim 15 - 20 \times 10^6$ positron events for each data point. The μSR data were analyzed by using the Musrfit software package.[8]

A. Analysis of $\lambda^{-2}(T)$ dependencies

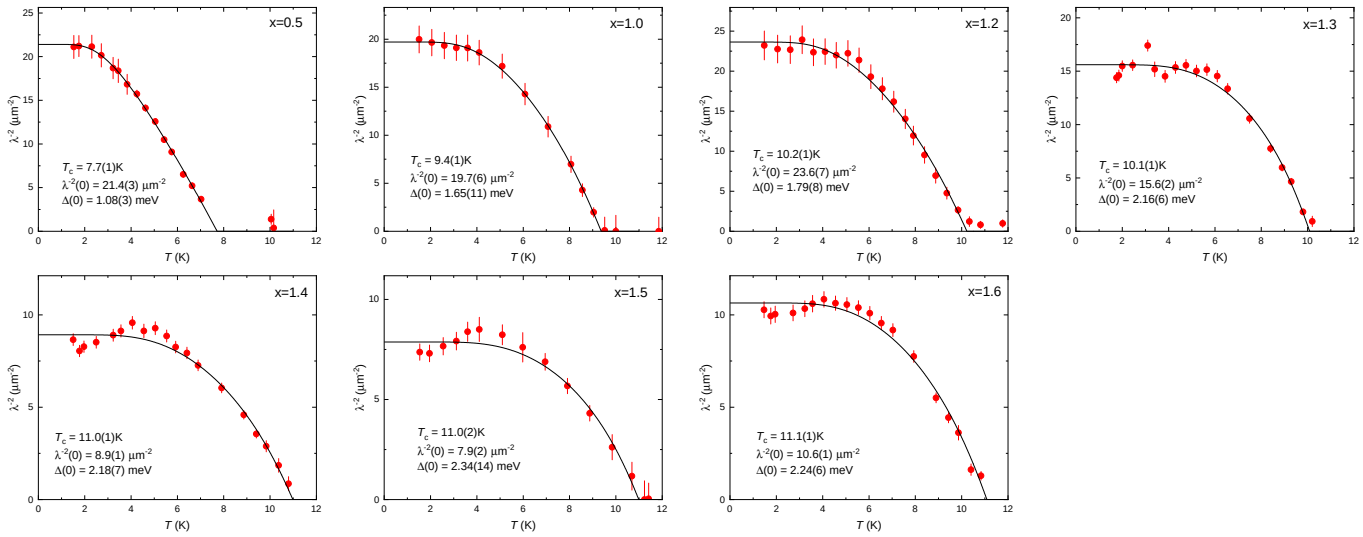

FIG. 5: Temperature dependencies of the inverse squared magnetic penetration depth λ^{-2} of $Mo_5Si_{3-x}P_x$ as they obtained in TF-μSR experiments. The solid lines are fits of Eq. 3 from the main text to $\lambda^{-2}(T)$ data. The fit parameters, namely the superconducting transition temperature T_c, the zero temperature value of the inverse squared magnetic penetration depth $\lambda^{-2}(0)$, and the superconducting energy gap $\Delta(0)$, are presented at each corresponding panel.

The individual temperature dependencies of the inverse squared magnetic penetration depth λ^{-2} of $Mo_5Si_{3-x}P_x$, as they obtained in TF-μSR experiments, are presented in Fig. 5. The parameters obtained from the fit of the $s-$wave gap model (Eq. 3 in the main text) to $\lambda^{-2}(T)$ data, namely the superconducting transition temperature T_c, the zero

temperature value of the inverse squared magnetic penetration depth $\lambda^{-2}(0)$, and the superconducting energy gap $\Delta(0)$, are shown at the corresponding panels.

VIII. ZERO-FIELD μSR MEASUREMENTS

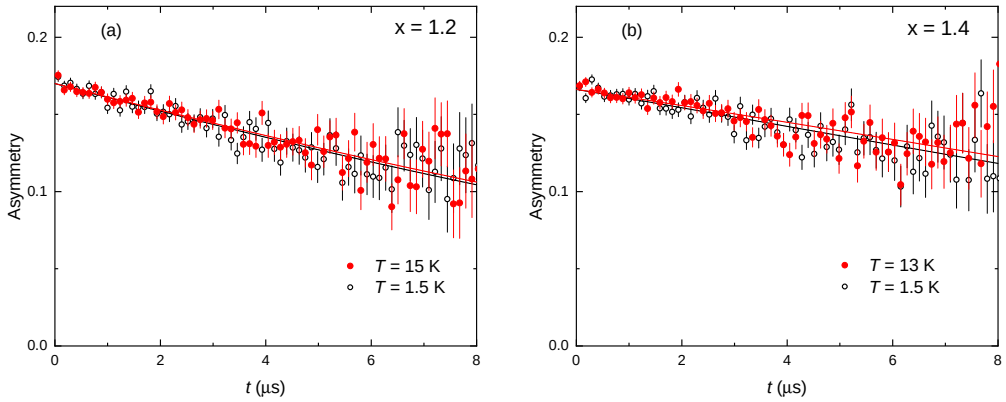

FIG. 6: Representative ZF-μSR time-spectra in the normal and the superconducting state of $x = 1.2$ and $x = 1.4$ $Mo_5Si_{3-x}P_x$ samples. The solid lines are fits of Eq. 5 to the data.

The zero-field μSR measurements were performed in order to reveal a possible breaking of the time-reversal symmetry, which may indicate an unconventional superconducting state of $Mo_5Si_{3-x}P_x$ system. The ZF-μSR time spectra for $x = 1.2$ and $x = 1.4$ samples, collected above the superconducting transition temperature T_c and at $T \simeq 1.5$ K, are presented in Fig. 6. Neither coherent oscillations nor fast decays could be seen thus excluding any type of magnetic order or fluctuations.

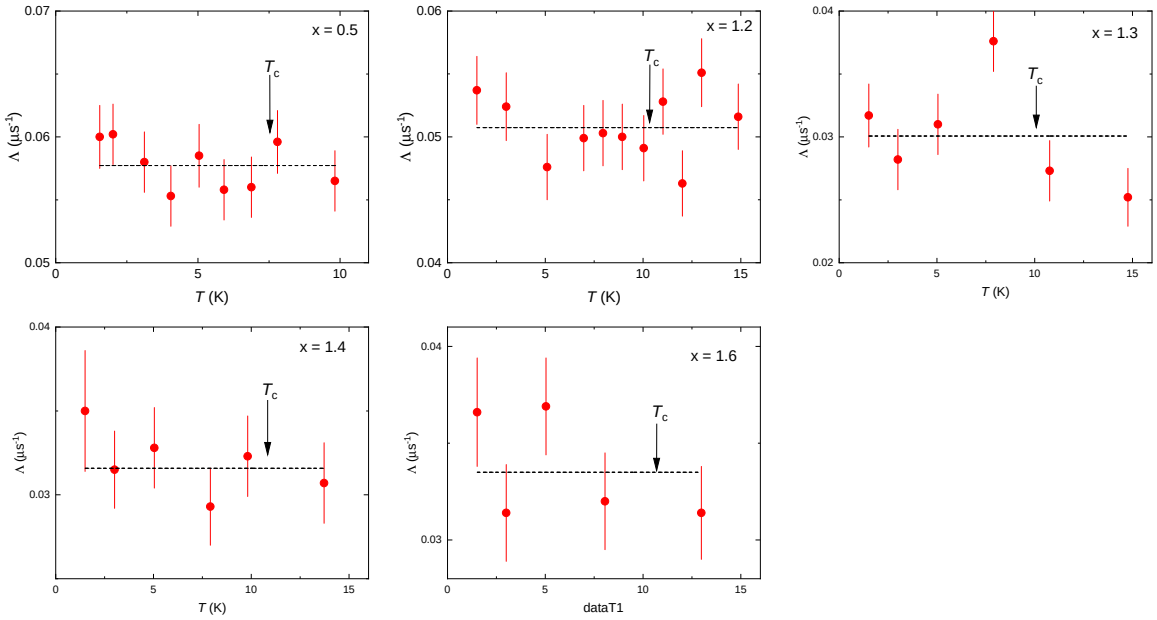

FIG. 7: Temperature dependencies of the exponential relaxation rate Λ of $Mo_5Si_{3-x}P_x$ as obtained in ZF-μSR experiments.

The zero-field μSR spectra were fitted using the Gaussian Kubo-Toyabe (GKT) relaxation function,[8,9] describing the nuclear moment response, multiplied by an additional exponential term:

$$A(t) = A_0 \left[\frac{1}{3} + \frac{2}{3}(1 - \sigma_{\mathrm{GKT}}^2 t^2)\, e^{-\sigma_{\mathrm{GKT}}^2 t^2/2} \right] e^{-\Lambda t}. \quad (5)$$

Here, A_0 is the initial asymmetry, σ_{GKT} is the GKT relaxation rate, and Λ is the exponential relaxation rate. In the above equation, σ_{GKT} accounts for the nuclear moment contribution, which is assumed to be static within the μSR time window and independent on temperature.

Figure 7 shows the temperature dependence of the exponential relaxation rate Λ of $Mo_5Si_{3-x}P_x$ samples. The absence of an additional μSR relaxation below T_c excludes a possible time-reversal symmetry breaking in the superconducting state of $Mo_5Si_{3-x}P_x$.

* Electronic address: rustem.khasanov@psi.ch
† Electronic address: bbruan@mail.ustc.edu.cn

[1] Bin-Bin Ruan, Jun-Nan Sun, Yin Chen, Qing-Song Yang, Kang Zhao, Meng-Hu Zhou, Ya-Dong Gu, Ming-Wei Ma, Gen-Fu Chen, Lei Shan, Zhi-An Ren, *Strong-coupling superconductivity with $T_c \sim 10.8$ K induced by P doping in the topological semimetal Mo_5Si_3*. Sci. China Mater. **65**, 3125 (2022).
https://doi.org/10.1007/s40843-022-2102-8

[2] Paolo Giannozzi, Stefano Baroni, Nicola Bonini, Matteo Calandra, Roberto Car, Carlo Cavazzoni, Davide Ceresoli, Guido L. Chiarotti, Matteo Cococcioni, and Ismaila Dabo1, *QUANTUM ESPRESSO: a modular and open-source software project for quantum simulations of materials*. J Phys: Condens Matter **21** 395502 (2009).
https://doi.org/10.1088/0953-8984/21/39/395502

[3] J. P. Perdew, K. Burke, M. Ernzerhof, *Generalized Gradient Approximation Made Simple*, Phys. Rev. Lett., **77**, 3865 (1996).
https://doi.org/10.1103/PhysRevLett.77.3865

[4] M. Schlipf, F. Gygi, *Optimization algorithm for the generation of ONCV pseudopotentials*, Comput. Phys. Commun., **196**, 36 (2015).
https://doi.org/10.1016/j.cpc.2015.05.011

[5] B. H. Toby, *EXPGUI, a graphical user interface for GSAS*, J. Appl. Crystallogr, **34**, 210 (2001).
https://doi.org/10.1107/S0021889801002242

[6] W. L. McMillan, **Transition Temperature of Strong-Coupled Superconductors**, Phys. Rev. **167**, 331 (1968).
https://doi.org/10.1103/PhysRev.167.331

[7] A. Amato, H. Luetkens, K. Sedlak, A. Stoykov, R. Scheuermann, M. Elender, A. Raselli, and D. Graf, *The new versatile general purpose surface-muon instrument (GPS) based on silicon photomultipliers for μSR measurements on a continuous-wave beam*. Rev. Sci. Instrum. **88**, 093301 (2017).
https://doi.org/10.1063/1.4986045

[8] A. Suter and B. M. Wojek, *Musrfit: A Free Platform-Independent Framework for μSR Data Analysis*, Phys. Procedia **30**, 69 (2012).
https://doi.org/10.1016/j.phpro.2012.04.042

[9] R. S. Hayano, Y. J. Uemura, J. Imazato, N. Nishida, T. Yamazaki, and R. Kubo. *Zero-and low-field spin relaxation studied by positive muons*. Phys. Rev. B **20**, 850 (1979).
https://doi.org/doi:10.1103/PhysRevB.20.850